Title
A MULTIPERIPHERAL BOOTSTRAP MODEL

Authors
Chew, G.F.
Pignotti, A.

Publication Date
1968-06-05

University of California

Ernest O. Lawrence Radiation Laboratory

A MULTIPERIPHERAL BOOTSTRAP MODEL

G. F. Chew and A. Pignotti

June 5, 1968

Berkeley, California

Submitted to Physical Review

UCRL-18275
Preprint

UNIVERSITY OF CALIFORNIA

Lawrence Radiation Laboratory
Berkeley, California

AEC Contract No. W-7405-eng-48

A MULTIPERIPHERAL BOOTSTRAP MODEL

G. F. Chew and A. Pignotti

June 5, 1968

A MULTIPERIPHERAL BOOTSTRAP MODEL*

G. F. Chew and A. Pignotti

Lawrence Radiation Laboratory
University of California
Berkeley, California

June 5, 1968

ABSTRACT

A crude bootstrap model is constructed, based on forward-direction unitarity and the multi-Regge hypothesis. The Pomeranchuk trajectory is generated by iteration of lower meson trajectories, whose average residue is correlated with average trajectory height. Iteration of the Pomeranchuk turns out to be a small but nonvanishing perturbation that requires the effective average height of the Pomeranchuk to be slightly less than 1. The model yields a two-parameter formula for multiple-production cross sections that agrees satisfactorily with nucleon-nucleon data up to 30 GeV.

A. INTRODUCTION

The qualitative success of the Regge-pole hypothesis for high-energy reactions with two-hadron final states requires serious attention to the multi-Regge hypothesis for multiple production.[1] One may here be motivated simply by the desire to correlate high-energy experimental data or by the deeper impulse to understand something about the role of multiparticle unitarity in the hadronic bootstrap. The hadron bootstrap supposes the existence of a unique analytic relativistic S matrix in which all poles are Regge poles, an S matrix that approximates the actual behavior of hadrons, the principal error being the neglect of electromagnetism. The nonlinearity of the unitarity condition has frustrated, and will continue to frustrate, theoretical attempts to construct a complete S matrix satisfying all bootstrap conditions. (It is not even certain that such a matrix exists.) The only recourse for theorists at present seems to cheat--peeking at experiments to get hints of the mechanism by which nature has achieved self-consistency. By this approach theorists have in the past discovered certain small ratios upon which rough models for limited regions of the S matrix can be based, the incomplete character of the models being manifested by a number of arbitrary parameters. This paper describes one such model--dealing with the multiperipheral region--that is, high energies and low momentum-transfers.

It is characteristic of bootstrap model construction that the number of arbitrary parameters is not apparent at the beginning of the task, nor is the degree of self-consistency that will be achieved. One might state as the bootstrap principle: The greater the model's consistency, the fewer the parameters. The model to be constructed in this paper is crude and contains three or four parameters. A remarkable feature, however, is that by the unitarity constraint the magnitudes of certain pole residues (or coupling constants) turn out to be determined by the location of trajectories. The model bases its rough self-consistency on three small quantities with the dimensions of energy: Taking 1 GeV as a "characteristic" hadronic energy, the pion mass may be considered small and so may the mean momentum transfer in a high-energy collision. The third small quantity on which we shall lean heavily is the slope of the Pomeranchuk trajectory.

Unitarity is employed only through the optical theorem, relating the total cross section to the imaginary part of the forward elastic amplitude. We make no attempt to satisfy unitarity at nonforward directions or in inelastic processes. We also largely ignore analyticity properties in momentum transfers. Inclusion of such constraints is an obvious objective for future improvement of this type of model.

A prerequisite for our model is Dolen-Horn-Schmid duality,[2] which we assume justifies a rough multi-Regge description of high-energy multiple production that ignores resonance production and concentrates on those final particles that are stable with respect to strong interactions. We further assume that in addition to the Pomeranchuk the most important trajectories are those containing the least massive hadrons, the 0^- and 1^- mesons, together with their exchange degenerate partners whose first physical points are 1^+ and 2^+. It follows that at the internal vertices in a multiperipheral "chain" only 0^- mesons are emitted with appreciable probability. For the same reason, at end vertices baryon number tends to be conserved. Thus the bulk of any high-energy reaction amplitude should be representable by diagrams of the type of Fig. 1.

For simplicity, in most of this paper we shall pretend there is only one kind of stable meson. Appeal to SU_3 might improve the model, but we wish to avoid indices that obscure essential features. At the same time two different types of meson trajectory must be recognized. For a fixed final multiplicity, Pomeranchuk exchange inevitably dominates at sufficiently large total energy. We shall see, however, that the bulk of the <u>total</u> inelastic cross section at any given energy is dominated by lower trajectories. In our model we combine the effect of all lower meson trajectories into a single trajectory.

At this stage, then, the model contains two trajectories α_P and α_M and two internal vertex functions, f_M representing the vertex of Fig. 2(a) and f_P representing that of Fig. 2(b). Each internal vertex function depends on the two adjacent momentum transfers as well as the Toller angle; but subsequent approximations will integrate over these variables and reduce the discussion to "vertex constants", g_M and g_P. The other parameters of the model are associated with the end vertices. Again by integration these will be representable by constants, G_M and G_P.

Consistent with forthcoming approximations that will average over momentum transfers, we shall neglect the slopes of the trajectories α_P and α_M and employ average (constant) values of these quantities. At such a stage, therefore, our model will contain a total of six real parameters for a definite choice of initial particles; only two of these parameters, G_M and G_P, depend on the initial particles. Unitarity will turn out to require

$$g_M{}^2 \approx 2(1 - \alpha_M)$$

and

$$g_P{}^2 \lesssim 2(1 - \alpha_P) \quad ,$$

a limit so small that for many purposes $g_P{}^2$ can be set equal to zero and α_P equal to 1, leaving only three parameters. The magnitudes of elastic and total cross sections will determine G_M and G_P, and all questions of energy dependence and multiplicity distribution will devolve onto the one remaining parameter.

The model studied here is similar in many ways to a model of Chan, Łoskiewicz, and Allison,[3] which includes two different meson trajectories as well as a baryon trajectory, and which is designed to describe individual reactions, rather than to investigate bootstrap constraints. We are encouraged by the success of the Chan-Łoskiewicz-Allison model, but for us to include so many trajectories would preclude simple closed forms for total cross sections and obscure the essential bootstrap aspects of the problem.

B. KINEMATICAL PRELIMINARIES

The cross section for production of n mesons when particle a collides with particle b may be written

$$d\sigma_n^{ab} = \frac{1}{\sinh \eta_0} \left| A_n^{ab} \right|^2 d\,\Phi_n \quad , \tag{B.1}$$

where

$$\cosh \eta_0 = \frac{s - m_a^2 - m_b^2}{2m_a m_b} \tag{B.2}$$

if s is the total center-of-mass energy squared. In terms of Toller variables the phase space $d\Phi_n$ is[4]

$$d\Phi_n = \cosh q_a \cosh q_b \prod_{j=1}^{n} \sinh q_j \, d\omega_j \prod_{i=1}^{n+1} dt_i \, d \cosh \xi_i \, \frac{\delta(\cosh \eta - \cosh \eta_0)}{\sinh \eta_0} \quad . \tag{B.3}$$

In this expression there is, for each internal vertex j, an angle ω_j and a boost q_j given by

$$\cosh q_j = \frac{\mu^2 - t_j - t_j'}{2(-t_j)^{\frac{1}{2}}(-t_j')^{\frac{1}{2}}} \quad , \tag{B.4}$$

where t_j and t_j' are the invariant squares of the momentum transfers adjacent to the j'th vertex. The end vertices have no associated angles, and the boosts are given by

$$\cosh q_a = (1 - t_1/4m_a^{\,2})^{\frac{1}{2}}$$

$$\cosh q_b = (1 - t_{n+1}/4m_b^{\,2})^{\frac{1}{2}}. \qquad \text{(B.5)}$$

In (B.3) the variable ξ_i is a boost associated with the i'th momentum transfer and is related to the corresponding two-particle subenergy squared by

$$s_i = t_{i-1} + t_{i+1} + 2(-t_{i-1})^{\frac{1}{2}}(-t_{i+1})^{\frac{1}{2}}$$

$$\times [\sinh q_{i-1} \sinh q_i \cosh \xi_i + \cosh q_{i-1} \cosh q_i] . \qquad \text{(B.6)}$$

The quantity η depends on all $3n + 2$ Toller variables, but the dependence factorizes when each ξ_i is large:

$$\cosh \eta \approx \cosh q_a \cosh q_b \prod_{j=1}^{n} (\cosh q_j + \cos \omega_j) \prod_{i=1}^{n+1} \cosh \xi_i \quad . \qquad \text{(B.7)}$$

Let us now define

$$\lambda_i \equiv [\cosh q_{i-1} + \cos \omega_{i-1}]^{\frac{1}{2}} [\cosh q_i + \cos \omega_i]^{\frac{1}{2}} \qquad \text{(B.8)}$$

and

$$e^{x_i} \equiv \lambda_i \cosh \xi_i \quad . \qquad \text{(B.9)}$$

Then the constraint (B.7) becomes

$$X_0 = \sum_{i=1}^{n+1} x_i , \tag{B.10}$$

if

$$e^{X_0} = \frac{\cosh \eta}{[\cosh q_a \cosh q_b]^{\frac{1}{2}}} . \tag{B.11}$$

At the same time the phase space (B.3) becomes

$$d\Phi_n = \frac{1}{\sinh \eta_0} \prod_{j=1}^{n} \frac{\sinh q_j \, d\omega_j}{\cosh q_j + \cos \omega_j} \prod_{i=1}^{n+1} dt_i \, dx_i \, \delta(X_0 - \sum_i x_i) . \tag{B.12}$$

According to (B.10) the lower limit on x_i is $\log \lambda_i$; but if the outgoing meson mass squared is smaller than or of the same order as the average t, the quantity λ_i is on the average of order unity, regardless of the values taken by the angles ω_j. We are thus led to make the basic and greatly simplifying assumption that the lower limit for any x_i is zero.

The preceding formulas are general, simply representing kinematics. Multiperipheralism is injected by assuming for the production amplitude A_n the factored form,

$$A_n^{ab} \sim \mathcal{F}_a(t_1)\,\mathcal{F}_b(t_{n+1}) \prod_{j=1}^{n} \mathcal{F}_j(t_j,\ t_{j+1},\ \omega_j) \prod_{i=1}^{n+1} (\cosh \xi_i)^{\alpha_i(t_i)} , \qquad \text{(B.13)}$$

with the vertex functions $\mathcal{F}$ large only for small values of the t's.

Substituting (B.13) and (B.12) into (B.1) and integrating over the $d\omega$'s, we have

$$d\sigma_n^{ab} = e^{-2X_0}\,\delta(X_0 - \sum_i x_i)\, f_a^2(t_1)\, f_b^2(t_{n+1}) \prod_{j=1}^{n} f_j^2(t_j,\ t_{j+1}) \prod_{i=1}^{n+1} dt_i\, dx_i\, e^{2\alpha_i x_i} , \qquad \text{(B.14)}$$

where f_j^2 is the product of $|\mathcal{F}_j(t_j,\ t_{j+1},\ \omega_j)|^2$ and known functions of the same three variables, integrated over $d\omega_j$.

C. THE MODEL

As explained in the introduction, the model includes two trajectories, to be labeled P (for Pomeranchuk) and M (for meson). Interference between P and M for the same momentum transfer will be ignored on the basis that large values of a particular s_i will be dominated by P and small values by M. Internal degrees of freedom, such as charge, of the actual outgoing mesons also help to wash out interference effects.

There are thus two different "end-vertex" functions, $f_{aP}^{\,2}(t)$ and $f_{aM}^{\,2}(t)$, and two different "internal-vertex" functions, $f_{MM}^{\,2}(t, t')$ and $f_{MP}^{\,2}(t, t')$. A basic assumption of the model is that we can approximate the integral of the internal vertex functions over the kinematically allowed region of momentum transfers in the following way

$$\int f_a^{\,2}(t_1)\, dt_1\, f_1^{\,2}(t_1, t_2)\, dt_2 \cdots f_n^{\,2}(t_n, t_{n+1})\, dt_{n+1}\, f_b^{\,2}(t_n)$$

$$\approx G_{ax}^{\;2}\, g_M^{\;2i}\, g_P^{\;2(n-i)}\, G_{by}^{\;2} \quad . \qquad (C.1)$$

Here x and y represent the first and the last Regge poles exchanged, and stand for either P or M. The exponent i is the number of times that an internal vertex of the type shown in Fig. 2(a) occurs; and, correspondingly, n - i is the number of internal vertices of the type shown in Fig. 2(b). Equation (C.1) follows if the integrations over the t's are performed between minus infinity and zero, and the vertex functions have the form

$$f_i(t_i, t_{i+1}) = g_i f(t_i) f(t_{i+1}) \quad ,$$

$$f_a(t_1) = G_{ax} f(t_1) \quad , \qquad (C.2)$$

and

$$f_b(t_{n+1}) = G_{by} f(t_{n+1}) \quad ,$$

where g_i, G_{ax}, and G_{by} are constants depending on the nature of the lines linked at the vertex and $f(t)$ is an arbitrary universal momentum transfer dependence. Finally, we replace $\alpha_i(t_i)$ by a suitable average value α_P or α_M when performing the t integrations in Eq. (B.14).

To illustrate the model, consider the diagram in Fig. 3, corresponding to the production of four mesons in a collision between particle a and particle b. In our model the cross section is given by

$$d\sigma_4^{aPMMPMb} \approx G_{aP}{}^2 G_{bM}{}^2 (g_P{}^2)^3 g_M{}^2 e^{2[\alpha_P x_1 + \alpha_M x_2 + \alpha_M x_3 + \alpha_P x_4 + \alpha_M x_5 - X_0]}$$

$$\times \; dx_1 \, dx_2 \, dx_3 \, dx_4 \, dx_5 \, \delta(X_0 - x_1 - x_2 - x_3 - x_4 - x_5) \, . \qquad (C.3)$$

We ignore Bose statistics because the regions of phase space occupied by different outgoing mesons tend not to overlap. Furthermore, if we alter the ordering of M and P trajectories in the chain, we populate a different region of phase space. In other words, each linear arrangement of P and M trajectories gives a separate additive contribution to the cross section. Observe that, as emphasized in the introduction, only two of our six parameters depend on the initial particle types.

D. TOTAL CROSS SECTIONS: THE OPTICAL THEOREM AS A BOOTSTRAP CONDITION

Let us begin the bootstrap analysis with the subset of peripheral diagrams containing only meson trajectories. Designating by $\sigma_n^{aM\cdots Mb}$ the associated cross section for production of n mesons, our model gives

$$d\sigma_n^{aM\cdots Mb} = G_{aM}^2\, G_{bM}^2 (g_M^2)^n\, e^{2(\alpha_M-1)X_0}\, dx_1\, dx_2 \cdots dx_{n+1}$$

$$\times\ \delta(x_1 + \cdots x_{n+1} - X_0)\ , \qquad \text{(D.1)}$$

or, after integration over the dx_i,

$$\sigma_n^{aM\cdots Mb} = G_{aM}^2\, G_{bM}^2\, \frac{(g_M^2\, X_0)^n}{n!}\, e^{(2\alpha_M-2)X_0}\ . \qquad \text{(D.2)}$$

We tentatively assume this Poisson distribution in n to sufficiently depress high multiplicities so that (D.2) yields a negligible contribution from $n \gtrsim [(s)^{\frac{1}{2}} - m_a - m_b]/\mu$, where the model must fail. It is then physically meaningful to sum (D.2) over all n, obtaining

$$\sigma_{tot}^{aM\cdots Mb} = G_{aM}^2\, G_{bM}^2\, e^{(2\alpha_{M'}-2)X_0}, \text{ with } 2\alpha_{M'} = 2\alpha_M + g_M^2\ . \qquad \text{(D.3)}$$

Since $e^{X_0} \sim s$, the Froissart limit prohibits $\alpha_{M'}$ from being greater than 1 and thus g_M^2 from being greater than $2(1 - \alpha_M)$. This unitarity limitation on the magnitude of a coupling constant is a crucial aspect of the bootstrap. Analysis of self-consistency will be seen below to convert the upper limit on g_M^2 into a rough equality.

The upper limit is already sufficient to justify <u>a posteriori</u> our having neglected the energy conservation constraint on multiplicity. By a short calculation, the average number of mesons within the distribution (D.2) is found to be

$$\bar{n}^{aM\cdots Mb} = g_M^2 X_0 \quad , \tag{D.4}$$

the single parameter g_M^2 controlling multiplicity.

The result (D.3) may evidently be generalized into the following contraction rule: The cross section from summing over all numbers of M trajectories occurring either between two P trajectories, between a P trajectory and an end-vertex, or between the two end-vertices (as in D.3), is obtained by replacing the "cluster" of M trajectories with a single new trajectory at $\alpha_{M'} = \alpha_M + g_M^2/2$. The general problem is thereby reduced to one of alternating P and M' trajectories, with internal vertex constants all equal to g_P^2.

The total cross section is thus composed of four parts:

$$\sigma_{tot}^{ab} = \sigma_{tot}^{aP\cdots Pb} + \sigma_{tot}^{aP\cdots M'b} + \sigma_{tot}^{aM'\cdots Pb} + \sigma_{tot}^{aM'\cdots M'b} \quad , \tag{D.5}$$

proportional respectively to $G_{aP}^2\, G_{bP}^2$, $G_{aP}^2\, G_{bM}^2$, $G_{aM}^2\, G_{bP}^2$ and

$G_{aM}^{\ 2}\ G_{bM}^{\ 2}$; and the optical theorem relates this sum to the imaginary part of the forward elastic amplitude, which we suppose to be dominated by the Pomeranchuk trajectory with $\alpha_P(0) = 1$. Thus our basic bootstrap requirement is that at high energy (D.5) should approach a nonvanishing constant. Let us examine separately each of the four components. Denoting by $\sigma_N^{aP\cdots Pb}$ the cross section for both end vertices to be connected to P trajectories, with N intermediate clusters as shown in Fig. 4, we have

$$\sigma_N^{aP\cdots Pb} = G_{aP}^{\ 2}\ G_{bP}^{\ 2}(g_P^{\ 2})^{2N}\ e^{2(\alpha_P-1)X_0} \int_0^{X_0} dz\, \frac{z^{N-1}}{(N-1)!} \times \frac{(X_0 - z)^N}{N!}\, e^{-2(\alpha_P-\alpha_{M'})z} \quad . \tag{D.6}$$

We are unable to give a general closed form for the sum of (D.7) over N, that is, for $\sigma_{tot}^{aP\cdots Pb}$; but we shall find the total cross section consistency requirement to demand that $\alpha_{M'}$ be close to α_P, in which case an approximate closed form can be obtained. The Froissart limit on $\sigma_{tot}^{aP\cdots Pb}$ so severely constrains the magnitude of $g_P^{\ 2}$, given α_P close to 1, that repetition of the Pomeranchuk trajectory is highly improbable. Most of the inelastic cross section then must arise from chains containing no Pomeranchuk trajectories, whose sum is given by (D.3). Since the total inelastic cross section must be approximately independent of energy, it follows that $\alpha_{M'} \approx 1$. If α_P and $\alpha_{M'}$ are so close to each other that $|\alpha_P - \alpha_{M'}|X_0 << 1$, one can easily derive that

$$\sigma_{tot}^{aP\cdots Pb} \approx G_{aP}^{\ 2}\, G_{bP}^{\ 2}\, e^{(\alpha_P+\alpha_{M'}-2)X_0} \cosh(g_P^{\ 2}\, X_0) \quad . \tag{D.7}$$

Evidently if we do not want the total cross section to increase in this region, we must demand

$$g_P^{\ 2} \leqslant 2 - \alpha_P - \alpha_{M'} \quad , \tag{D.8}$$

which exhibits the above-mentioned smallness of $g_P^{\ 2}$.

Looking next at the contribution where the a vertex connects to P and the b vertex to M', we find

$$\sigma_N^{aP\cdots M'b} = G_{aP}^{\ 2}\, G_{bM}^{\ 2} (g_P^{\ 2})^{2N+1}\, e^{2(\alpha_P-1)X_0} \int_0^{X_0} dz\, \frac{z^N}{N!} \frac{(X_0 - z)^N}{N!}$$

$$\times \quad e^{-2(\alpha_P-\alpha_{M'})z} \quad , \tag{D.9}$$

where now N has the significance shown in Fig. 5. If $\alpha_{M'}$ is close to α_P in the above sense,

$$\sigma_{tot}^{aP\cdots M'b} \approx G_{aP}^{\ 2}\, G_{bM}^{\ 2}\, e^{(\alpha_P+\alpha_{M'}-2)} \sinh(g_P^{\ 2}\, X_0) \quad . \tag{D.10}$$

A similar result is obtained for the contribution where the a vertex connects to M' and the b vertex to P. Finally, the total cross section with M' at both ends of the chain is

$$\sigma_{tot}^{aM'\cdots M'b} \approx G_{aM}{}^2 G_{bM}{}^2 e^{(\alpha_P+\alpha_{M'}-2)} \cosh(g_P{}^2 X_0) \quad , \tag{D.11}$$

so that (D.5) becomes

$$\sigma_{tot}^{ab} \approx [(G_{aP}{}^2 G_{bP}{}^2 + G_{aM}{}^2 G_{bM}{}^2) \cosh(g_P{}^2 X_0) + (G_{aP}{}^2 G_{bM}{}^2 + G_{aM}{}^2 G_{bP}{}^2) \times \sinh(g_P{}^2 X_0)] e^{(\alpha_P+\alpha_{M'}-2)X_0} \quad , \tag{D.12}$$

if $|\alpha_P - \alpha_{M'}| X_0 \ll 1$. The desired constant high-energy limit follows if (D.8) becomes an equality, that is, if

$$g_P{}^2 = 2 - \alpha_P - \alpha_{M'} \quad . \tag{D.13}$$

Realizing that the elastic cross section in our model is

$$\sigma_{e\ell}^{ab} = G_{aP}{}^2 G_{bP}{}^2 e^{2(\alpha_P-1)X_0} \quad , \tag{D.14}$$

we rewrite (D.12) as

$$\sigma_{tot}^{ab} \approx \sigma_{e\ell}^{ab} [(1 + \gamma_a \gamma_b) \cosh(g_P{}^2 X_0) + (\gamma_a + \gamma_b) \sinh(g_P{}^2 X_0)] \times e^{(\alpha_{M'}-\alpha_P)X_0} \quad , \tag{D.12'}$$

where $\gamma_c = G_{cM}^2/G_{cP}^2$. It is also useful to identify the cross section for "diffractive dissociation" of particle b (see Formula D.9):

$$\sigma_{N=0}^{aPM'b} = G_{aP}^2 \, G_{bM}^2 \, g_P^2 \, e^{2(\alpha_P-1)X_0} \frac{1 - e^{-2(\alpha_P-\alpha_{M'})X_0}}{2(\alpha_P - \alpha_{M'})}$$

$$= \sigma_{e\ell}^{ab} \, \gamma_b \, g_P^2 \, \frac{1 - e^{-2(\alpha_P-\alpha_{M'})X_0}}{2(\alpha_P - \alpha_{M'})} \quad . \qquad (D.15)$$

For moderate lab energies and $\alpha_{M'}$ close to α_P, (D.15) can be approximated by

$$\sigma_{N=0}^{aPM'b} = \sigma_{e\ell}^{ab} \, \gamma_b (g_P^2 \, X_0) \quad . \qquad (D.15')$$

E. EXPERIMENTAL CONTENT OF THE 2-PARAMETER MODEL FOR THE INELASTIC CROSS SECTIONS WITH $g_P^2 = 0$

A simple version of our model sets $g_P^2 = 0$ and $\alpha_{M'} = \alpha_P = 1$. Recall that $g_M^2 = 2(1 - \alpha_M)$, and

$$\sigma_{e\ell}^{ab} \approx G_{aP}^2 \, G_{bP}^2 \ . \tag{E.1}$$

The total cross section (D.12') becomes

$$\sigma_{tot}^{ab} \approx (1 + \gamma_a \gamma_b) \, \sigma_{e\ell}^{ab} \ , \tag{E.2}$$

telling us immediately that $\gamma_a \approx 2$ if a refers to pions, kaons, or nucleons. The basic formula (D.2), now simplified to

$$\begin{aligned} \sigma_n^{ab} &\approx \gamma_a \gamma_b \, \sigma_{e\ell}^{ab} \frac{(g_M^2 X_0)^n}{n!} e^{-g_M^2 X_0} \\ &= \sigma_{tot\ inel}^{ab} \frac{(g_M^2 X_0)^n}{n!} e^{-g_M^2 X_0} \ , \end{aligned} \tag{E.3}$$

gives the cross section leading to the production of n mesons. This formula is supposed to describe the multiplicity and energy variation for all possible incident-particle combinations. For a given initial state it contains only two parameters: the coupling g_M^2 and the constant value of the total inelastic cross section $\sigma_{tot\ inel}^{ab}$. In the expression of X_0 as a function of the total energy squared s through Eqs. (B.2) and (B.11), we set

$$\cosh q_a \approx \cosh q_b \approx 1,$$

if the initial masses m_a and m_b are much larger than the average momentum transfer (such as in the nucleon-nucleon case). Otherwise, an additional parameter equal to the average momentum transfer may have to be introduced in Eq. (B.5).

In Appendix I we describe a confrontation of Eq. (E.3) with experimental values for proton-proton collisions. In this case we have

$$\sigma^{pp}_{\text{tot inel}} \approx 30 \text{ mb.} ,$$

and a reasonable success is achieved through the choice $g_M^2 \approx 1$. This corresponds to $\alpha_M \approx .5$, a plausible average height for meson trajectories. Note that the average number of mesons produced in an inelastic collision between any two hadrons is predicted by (D.4) to be approximately X_0.

F. THE MODEL WITH SMALL BUT NONVANISHING g_P^2

The so-called "diffractive-dissociation" cross section is predicted by (D.15) to be zero if $g_P^2 = 0$, but the experimental magnitude of diffractive-dissociation, while small, is nonvanishing. In proton-proton collisions, for example, a small and roughly constant cross section is observed for production of $N^*_{1/2}$ resonances of masses 1400, 1520, 1690, and 2190 MeV. Over a range of incident momenta between 10 and 30 GeV/c, the combined cross section for these processes is approximately equal to 1.5 mb. If we take this value as an estimate for the diffractive-dissociation cross section, Eq. (D.15') yields (after introducting a factor of 2 to allow for the possibility of diffractive-dissociation of either one of the initial particles)

$$g_P^2 \approx 0.02 \tag{F.1}$$

This number is sufficiently small as not to disturb the predictions discussed above in Sec. E, but it permits several interesting inferences. If

$$1 - \alpha_P \gtrsim 1 - \alpha_{M'} ,$$

then the order of magnitude of $1 - \alpha_P$ is given by g_P^2. This allows an estimate of the slope of the Pomeranchuk trajectory α'_P, since

$$\alpha'_P \, |\bar{t}| \approx 1 - \alpha_P, \tag{F.2}$$

if $\bar{t}$ is an average value of the momentum transfer squared. We are in this manner led to expect $g_P^2/|\bar{t}|$ as the order of magnitude of the Pomeranchuk slope, a number equal to 0.2 GeV^{-2} if $|\bar{t}|$ is taken as 0.1 GeV^2. The small value of the slope thus appears correlated with the small value of the internal Pomeranchuk coupling.[6]

The reader may well be puzzled as to why g_P^2 is so small compared to g_M^2 when G_{aP}^2 and G_{aM}^2 differ only by a factor ≈ 2. It seems required, after all, (referring back to (B.13)) that, when particle a happens to be a meson, the end-vertex function $\mathcal{F}_a(t_1)$ should be equal to the analytic continuation of an appropriate internal vertex function $\mathcal{F}_j(t_j, t_{j+1}, \omega_j)$, evaluated at $t_j = m_a^2$. Part of the explanation for the seeming paradox lies in the fact that many different meson trajectories are being represented in our model by α_M, and one expects the most important generally to be those whose first physical points correspond to unstable 1^- or 2^+ mesons, not the stable 0^- mesons which may couple at the end vertices. Note, however, that for the internal Pomeranchuk vertex of Fig. 2(b) the only important meson trajectory <u>is</u> likely to be that containing a 0^- meson of precisely the type emerging from the vertex. That is to say, by analytic continuation to a physical point on the M trajectory, Fig. 2(b) describes either elastic scattering or diffractive dissociation, depending on whether or not M and μ are identical mesons; it has been seen that diffractive dissociation is small compared to elastic scattering.

The upshot of the above reasoning is the absence of any simple relationship between G_{aM}^2 and g_M^2. At the same time we do expect a direct relation between G_{aP}^2 and g_P^2. Satisfaction of this relation is implicit in the success of calculations with the Deck model, which corresponds to Fig. 6 with the internal vertex taken to be a continuation of that which controls elastic π scattering on particle a.[7] The compatibility of this latter assumption with the small cross section for the process of Fig. 6 (a special example of diffractive dissociation) demonstrates the absence of any conflict between $g_P^2 \approx 0.02$ and the known values of pion elastic cross sections.

To sum up, once given the magnitude of a pion elastic cross section, multiperipheral bootstrap reasoning leads to a small value of g_P^2 and thereby makes plausible the small slope of the Pomeranchuk trajectory. At the same time, a zero slope is excluded. So far, of course, the Regge approach provides no explanation for the magnitude of an elastic cross section.

G. CONCLUSION

In the 1961 reasoning which led Chew and Frautschi to the Regge-pole hypothesis, a key element was a mechanism by which high-energy power behavior is achieved for a two-particle amplitude by an infinite sum of increasing powers of logarithms, each power of logarithm being associated with a particular inelastic multiplicity.[11] Their reasoning was motivated by the strip model and the analogous "ladder" mechanism by which Regge poles are generated through Mandelstam iteration in potential scattering. The same idea was explored further by Amati, Stanghellini and Fubini.[12] The ladder mechanism has constituted the basis for the present paper, but with the important distinction from early work that the "sides" of the ladder here consist of two Regge trajectories, rather than two individual hadrons. Furthermore it is complete unitarity in the direct reaction, not two-particle unitarity in the crossed reaction, that now provides the dynamics. The possibility of "laddering" a power through direct-reaction unitarity has previously been observed by Verdiev, et al.,[13] but with no attempt to construct a concrete model.

The approximate nature of the self-consistency achieved in the model of this paper cannot be emphasized too strongly. We are not proposing a way to avoid cuts in angular momentum, the phenomenon most often associated with a combination of two Regge trajectories. What we are proposing is that for reasonable energies it may be possible to approximate the actual amplitude by pure powers and to investigate on this basis a new kind of bootstrap contraint.

The reader may question our use of the adjective "bootstrap" to describe the model of this paper, since meson trajectories have here been employed only to generate the Pomeranchuk and not to generate themselves. Extension of forward unitarity to a charge-exchange reaction, however, would lead to a consistency requirement on the average Regge coupling strength analogous to that demanded here for elastic scattering. The difference is that the final power for a charge-exchange amplitude should correspond to α_M rather than to α_P. (A simple calculation reveals that such an objective is achieved if the average internal Regge coupling for the charge-exchange unitarity integral is half of that denoted in this paper by g_M^2.) Thus a simple extension of the basic considerations of this paper will lead to "self-generating" mechanisms for meson trajectories.

Appendix A.

We want here to confront the model described in this paper with some recent data for particle production in proton-proton collisions.[8,9] Before doing so, we should point out the unorthodoxy of our approach. In conventional multi-Regge analysis one usually chooses a particular process, performs various cuts in order to select the "pure" multi-Regge events, and tries to fit distributions corresponding to an integrated cross section of a few tenths of microbarns. Detailed fits of this type are of great interest, and we expect them to become more and more meaningful as more abundant experimental information becomes available. In contrast to this approach, we propose here to account in a gross way for most of the total inelastic cross section in an energy range from 12 to 29 GeV -- residing in inelastic events exhibiting between two and eight prongs. Although the two-parameter formula (E.3) depended on various averages and kinematic approximations, we take the fact of a reasonable fit as an indication that the multi-Regge model can account for the bulk of the inelastic cross section.

Because of the experimental difficulty in detecting neutral particles and in identifying charged particles, the data to be analyzed are expressed as cross sections for events characterized by a given number of final prongs. To translate the previous results into prongs, Eq. (E.3) must be augmented with a specification of the charges of the final particles. We assume for simplicity that only pions are produced and that the effective meson Regge pole has the following properties:

i) It carries either isospin zero or one,

ii) It occurs with equal probabilities at the ends of the multi-Regge chain with isospin zero and one.

iii) It occurs with alternating values of the isospin along the multi-Regge line.

As a consequence, two thirds of the pions produced will in average be charged. It also follows from the above assumptions that the inelastic cross section for processes with $2(i+1)$ prongs can be written

$$\sigma^{pp}_{2(i+1)\text{ prongs}} = \sum_{n=n_{min}(i)}^{\infty} \frac{1}{2}\left\{C[\mathrm{Int}(n/2),\ i] + C[\mathrm{Int}(\tfrac{n-1}{2}),\ i]\right\}\ \sigma^{pp}_{n}\ ,$$

where

$$n_{min}(i) = \text{Maximum}\ (2i,\ 1),$$

$$\mathrm{Int}(x) = \text{Integer part of}\ \ x,$$

$$C(m,\ i) = \begin{cases} (\frac{2}{3})^{i}\ (\frac{1}{3})^{m-i}\ \dfrac{m!}{i!\ (m-i)!} & \text{if}\quad m \geqslant i \\ 0 & \text{if}\quad m < i\ , \end{cases}$$

and σ^{pp}_{n} is given by Eq. (E.3).

In Table I we give the experimental values of the total inelastic cross section[10] and the cross sections for 4, 6, and 8 prongs,[8] at the five different energies used to check our model. We do not attempt to fit events with 10 or more prongs, for which threshold effects are likely to play a major role at the energies considered. A best fit to the experimental values gives for our parameters

$$\sigma^{pp}_{tot\ inel} = 29.7$$

and

$$g_M^{\ 2} = 1.14 \quad (\text{corresponding to } \alpha_M = .43)$$

The theoretical values for the cross sections are also given in Table I, where we include the prediction for the two-prong inelastic cross section, still unmeasured. We see that in spite of all our approximations, we come within 15% of the experimental value, except in the case of the comparatively smaller 8-prong cross section.

Having thus determined the parameters in our model, it is easy to make various kinds of predictions. As an example, we show in Table II the partial cross sections for production of one, two, and three pions predicted by our model at 28.5 GeV/c, compared with the experimental results by Connolly et al.[9] The agreement is good.

Table I. Total inelastic cross section, and inelastic cross sections for 2, 4, 6, and 8 prong events, at five values of the incident momentum for proton-proton collisions.

P_{Lab} GeV/c	$\sigma_{tot\ inel}$ mb.	$\sigma_{2\ pr.\ inel}$ mb.	σ_{4} prongs mb.	σ_{6} prongs mb.	σ_{8} prongs mb.
12.88	Ex: 29.0 Th: 29.7	Th: 11.2	Ex: 13.5 Th: 12.0	Ex: 4.1 Th: 4.5	Ex: 0.60 Th: 0.86
18.00	Ex: 29.7 Th: 29.7	Th: 9.7	Ex: 12.5 Th: 12.2	Ex: 5.2 Th: 5.6	Ex: 1.29 Th: 1.31
21.08	Ex: 29.9 Th: 29.7	Th: 9.0	Ex: 12.4 Th: 12.2	Ex: 6.2 Th: 6.1	Ex: 1.81 Th: 1.56
24.12	Ex: 29.9 Th: 29.7	Th: 8.5	Ex: 13.3 Th: 12.1	Ex: 7.1 Th: 6.5	Ex: 2.44 Th: 1.79
28.44	Ex: 29.8 Th: 29.7	Th: 7.9	Ex: 10.6 Th: 12.0	Ex: 6.4 Th: 6.9	Ex: 2.54 Th: 2.08

Table II. Predicted cross sections for production of one, two, and three pions in pp collisions at 28.5 GeV/c. The experimental values are from Ref. 9.

Final State	Predicted Cross Section (mb.)	Experimental Value (mb.)
$p\ n\ \pi^+$	1.44	$1.5 \pm .1$
$p\ p\ \pi^+\ \pi^-$	1.21	$1.1 \pm .2$
$p\ n\ \pi^+\ \pi^+\ \pi^-$	1.80	$1.6 \pm .3$

ACKNOWLEDGMENTS

We want to express our gratitude to Drs. Jared A. Anderson, Janos Kirz, Dennis B. Smith, and Robert Sprafka for having let us use their preliminary data prior to their publication. We are also indebted to Dr. Naren F. Bali for many helpful discussions during the early stages of this work.

FOOTNOTES AND REFERENCES

* This work was supported in part by the United States Atomic Energy Commission.

1. T. W. B. Kibble, Phys. Rev. 131, 2282 (1963).

K. A. Ter-Martirosyan, Soviet Phys. JETP 44, 341 (1963).

A. M. Popova and K. A. Ter-Martirosyan, Nuclear Phys. 60, 107 (1964).

Z. Koba, Fortschritte der Physik 11, 118 (1963).

I. G. Ivanter, A. M. Popova, and K. A. Ter-Martirosayn, Soviet Phys. JETP 19, 387 (1964).

K. A. Ter-Martirosyan, Nuclear Phys. 68, 591 (1964).

M. S. K. Razmi, Nuovo Cimento 31, 615 (1964).

I. A. Verdiev, A. M. Popova, and K. A. Ter-Martirosyan, Soviet Phys. JETP 19, 878 (1964).

I. A. Verdiev, O. V. Kancheli, S. G. Matinyan, A. M. Popova, and K. A. Ter-Martirosyan, Soviet Phys. JETP 19, 1148 (1964).

J. Joseph and H. Pilkuhn, Nuovo Cimento 33, 1407 (1964).

J. C. Polkinghorne, Nuovo Cimento 36, 857 (1965).

G. M. Fraser and R. G. Roberts, Nuovo Cimento 47, 339 (1967).

H. M. Chan, K. Kajantie, and G. Ranft, Nuovo Cimento 49, 157 (1967).

H. M. Chan, K. Kajantie, G. Ranft, W. Beusch, and E. Falminio, Nuovo Cimento 51, 696 (1967).

F. Zachariasen and G. Zweig, Phys. Rev. 160, 1322 (1967), and Phys. Rev. 160, 1326 (1967).

N. F. Bali, G. F. Chew, and A. Pignotti, Phys. Rev. 163, 1572 (1967).

K. Kajantie, Nuovo Cimento 53, 813 (1968).

J. Finkelstein and K. Kajantie, CERN TH857, preprint.

2. R. Dolen, D. Horn, and C. Schmid, Phys. Rev. 166, 1768 (1968);

G. F. Chew and A. Pignotti, Phys. Rev. Letters 20, 1078 (1968).

3. Chan Hong-Mo, J. Łoskiewicz, and W. W. M. Allison, CERN, TH 866 preprint, January, 1968.

4. N. F. Bali, G. F. Chew, and A. Pignotti, Phys. Rev. Letters 19, 614 (1967).

5. E. W. Anderson et al., Phys. Rev. Letters 16, 855 (1966).

6. J. Finkelstein and K. Kajantie have shown that violation of the Froissart limit results from multi-Pomeranchuk exchange [see Phys. Letters 26B, 305 (1968)]. Analysis of their result, however, reveals that the degree of violation is an order of magnitude more remote than the effects considered here. Our model requires major refinement before the tiny Finkelstein-Kajantie mechanism becomes significant. Moreover, a zero in the Pomeranchuk internal coupling when the momentum transfer of the Pomeranchuk line vanishes is enough to avoid the violation. If the conflict is resolved in this fashion, our model would still describe the integrated Pomeranchuk coupling by the non-vanishing constant g_P^2.

7. See E. Berger, Phys. Rev. 166, 1525 (1968), for a reggeized Deck calculation, and references to previous works. Note that Formula (D.15) corresponds to the cross section for the process of Fig. 6, summed over all possible b^*. The Deck model is usually applied to a particular b^* resonance.

8. J. Anderson, J. Kirz, D. Smith, and R. Sprafka, private communication.

9. P. L. Connolly et al., BNL 11980, preprint, presented at the Third Topical Conference on Resonant Particles, Athens, Ohio, November 1967.

10. The experimental value for the total inelastic cross section is obtained by subtracting the total elastic cross section from the total cross

section. The former is obtained by interpolation among the data reported in Fig. 1 of the compilation by G. Alexander, O. Benary, and U. Maor, Nucl. Physics B5, 1 (1968); the latter is chosen to be the fit by W. Rarita, R. J. Riddell Jr., C. B. Chiu, and R. J. N. Phillips, Phys. Rev. 165, 1615 (1968), which interpolates nicely the existing data.

11. G. F. Chew and S. C. Frautschi, Phys. Rev. 123, 1478 (1961).

12. D. Amati, A. Stanghellini and S. Fubini, Nuovo Cimento 26, 896 (1962).

13. I. A. Verdiev, O. V. Kancheli, S. G. Matinyan, A. M. Popova and K. A. Ter-Martirosyan, Soviet Phys. JETP 19, 1148 (1964).

FIGURE CAPTIONS

Fig. 1. Multiperipheral diagram for a "dominant" high-energy reaction. The symbol B denotes a stable baryon and μ a stable meson; M denotes a meson trajectory and P the Pomeranchuk trajectory.

Fig. 2. The two types of internal vertex in the model.

Fig. 3. A possible contribution to 4-meson production.

Fig. 4. The most general diagram with Pomeranchuk trajectories at both end-vertices, after contraction of meson trajectories.

Fig. 5. The most general diagram with a Pomeranchuk trajectory at vertex-a and a meson trajectory at vertex-b, after contraction of meson trajectories.

Fig. 6. Deck model for the reaction $a + b \rightarrow a + b^* + \pi$.

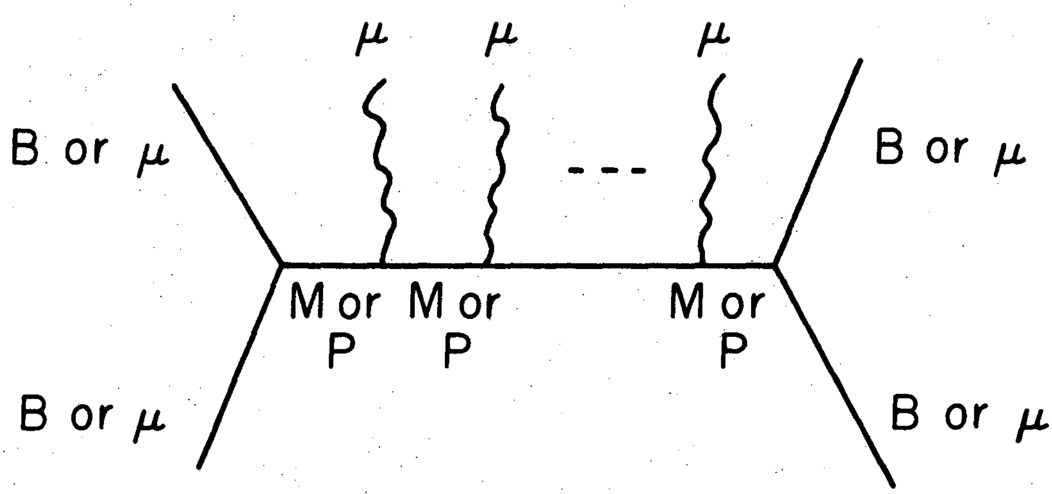

Fig. 1

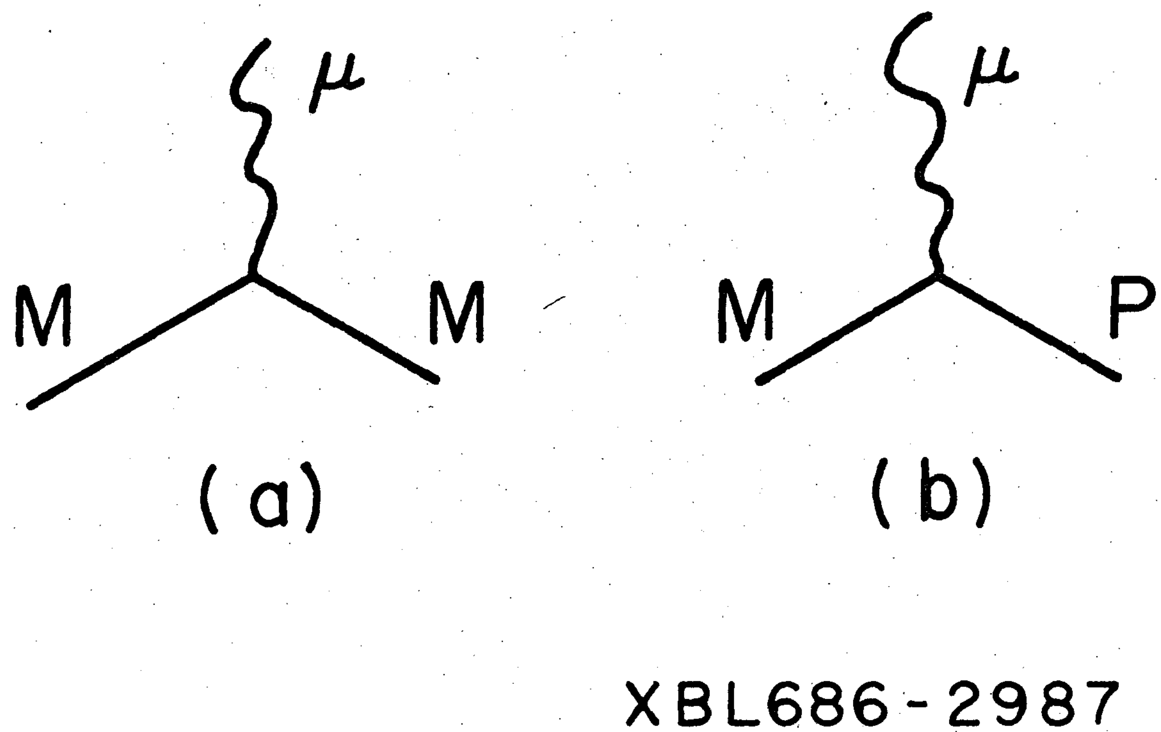

Fig. 2

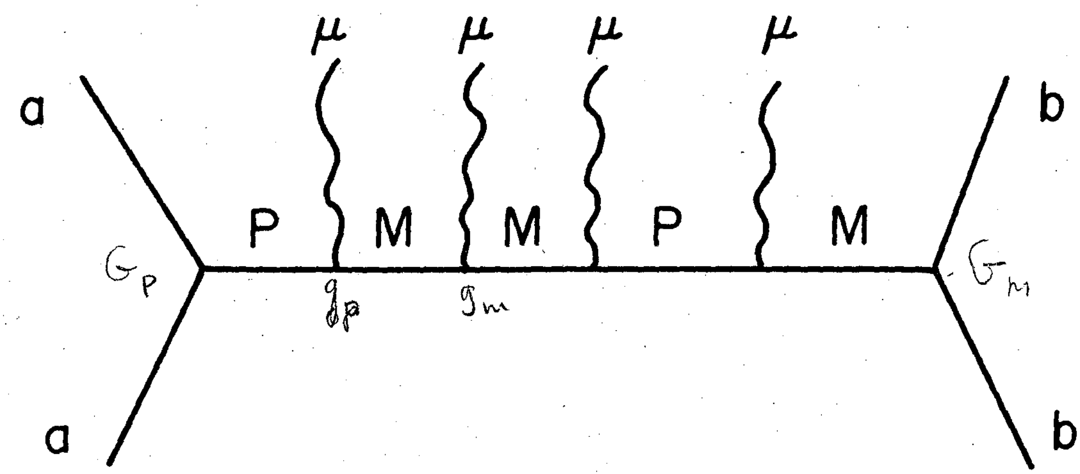

Fig. 3

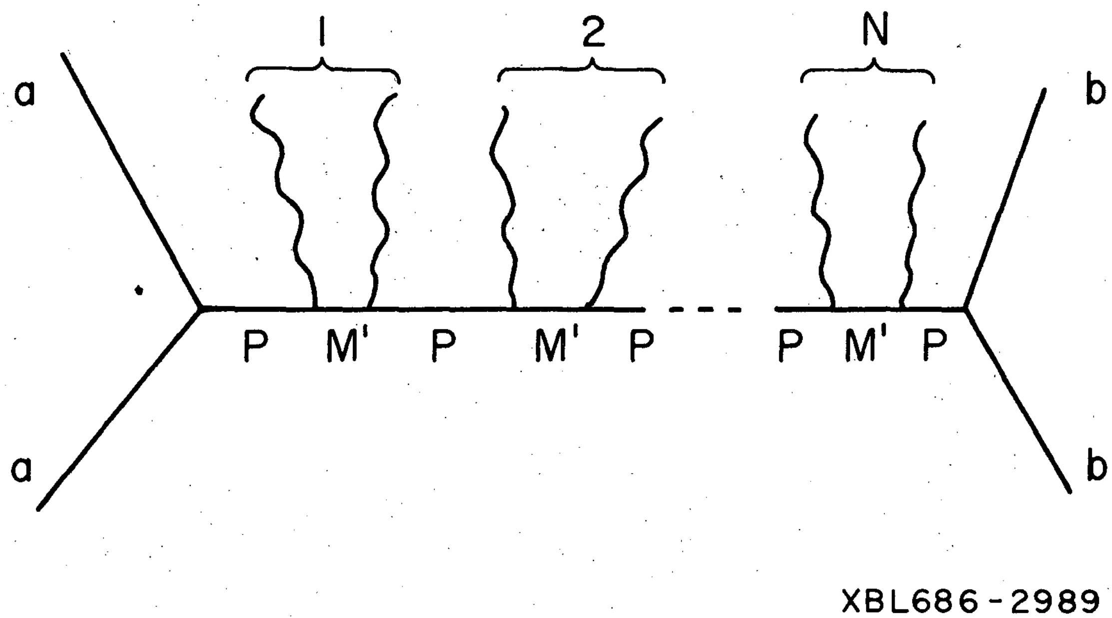

Fig. 4

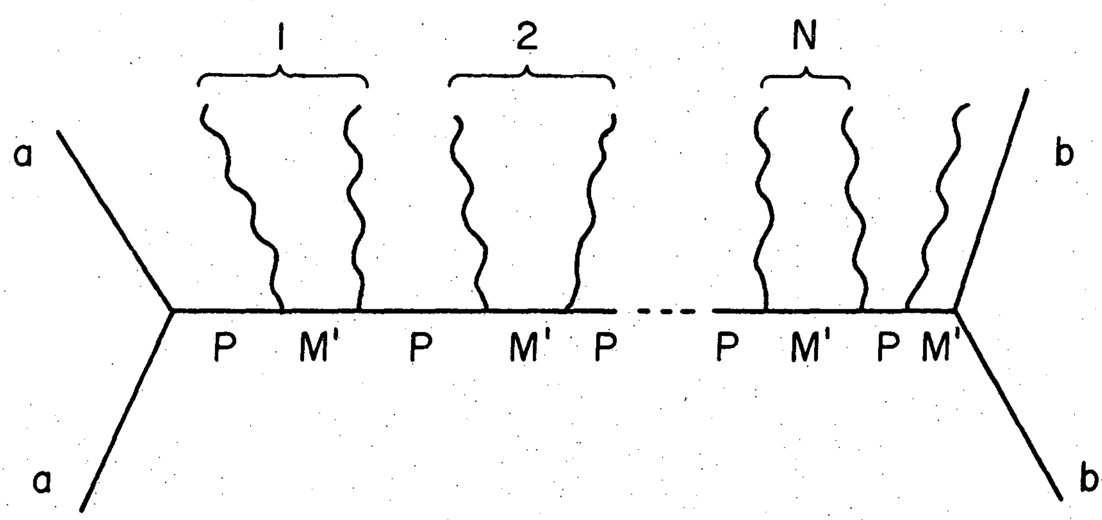

Fig. 5

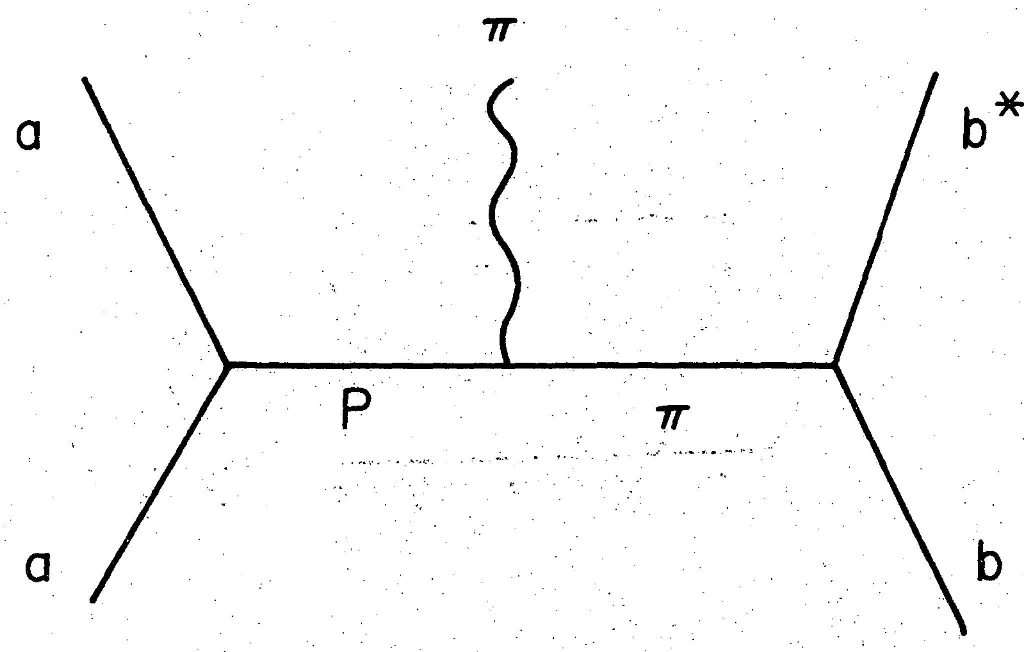

Fig. 6